

Comparison of carbon-ion passive and scanning irradiation
for pancreatic cancer
(膵癌に対する重粒子線パッシブ照射とスキヤニング照射の比較)

千葉大学院医学薬学府
先端医学薬学専攻
(主任：鎌田正教授)
塩見 美帆

Abstract

Purpose: To compare carbon-ion beam dose distribution between passive and scanning radiation therapies for locally advanced pancreatic cancer.

Materials and Methods: Thirteen pancreatic cancer patients were included in this study. Four types of treatment planning with respiratory gating were calculated for each patient: a four-field box with passive irradiation (Plan 1), scanning irradiation (Plan 2), a three-field (150°, 180° and 210°) protocol with passive irradiation (Plan 3), and scanning irradiation (Plan 4). The irradiation plans each delivered 55.2 Gy(RBE) to the planning target volume (PTV) and were compared with respect to doses to the PTV and organs at risk (OARs).

Results: Plan 3 exceeded the dose assessment metrics to the spinal cord. Scanning irradiation plans (Plan 2 and, particularly, Plan 4) offered significantly reduced dosage to the stomach and the duodenum compared with passive irradiation.

Conclusion: Three-field oblique scanning irradiation for pancreatic cancer has the potential to reduce gastrointestinal exposure and influence of peristalsis on dose distribution.

Keywords: Carbon-Ion Radiotherapy, Pancreatic Cancer, Radiation Dosimetry

INTRODUCTION

Pancreatic cancer accounted for an estimated 46,420 cancer cases and 39,590 cancer deaths worldwide in 2014 [1]. Selected patients may be curable when treated with high-dose chemoradiotherapy, but delivery of high-dose radiation is limited owing to the proximity of organs at risk (OARs). Several dosimetric studies have reported that proton therapy improves the dose-volume histograms (DVHs) over conventional photon therapy and intensity-modulated radiation therapy (IMRT) by reducing excessive doses to normal tissues [2, 3]. Carbon-ion beams provide a sharp lateral penumbra and narrow Bragg peak compared to proton beams [4], and demonstrate increased relative biological effectiveness (RBE).

Our carbon-ion beam therapy center was constructed in 1994, and has provided treatment to more than 9,000 cancer patients [5]. Since, a constant spread-out Bragg peak (SOBP) over the beam field in a passive irradiation system can cause undesirable doses to normal tissues at the beam entry side of the target, dose escalation can be limited by the risk of gastrointestinal side effects. The scanning delivery system was developed to avoid these issues. Our facility began providing scanning irradiation without respiratory gating in 2011, with good clinical results [6].

We have clinical experience with four-field box treatments for pancreatic cancer using passive irradiation. Before starting pancreatic scanning irradiation, it is necessary to evaluate dose distributions between passive and scanning irradiation techniques. Here, we compared dose distributions among irradiation techniques using treatment planning software.

MATERIALS AND METHODS

Between November 2013 and February 2014, 13 patients were randomly selected from among patients with inoperable pancreatic cancer who underwent four-field box passive irradiation at our hospital. The characteristics of the enrolled patients are listed in Table 1. The patients were positioned in customized cradles (Moldcare®, Alcare, Tokyo, Japan) and immobilized with a low-temperature thermoplastic shell (Shellfitter®, Kuraray, Osaka, Japan). Treatment planning CT was acquired in four-dimensional (4D) mode under free breathing conditions (Aquilion One Vision

Edition®, Toshiba Medical Systems, Otawara, Japan). The study was approved by the institutional review boards of our institutions and participating patients gave informed consent.

Treatment planning

Tumor extent was evaluated by CT, magnetic resonance imaging (MRI), and positron emission tomography (PET). A radiation oncologist manually delineated the gross tumor volume (GTV) and OARs on the CT images at peak exhale. Clinical target volume (CTV) was defined as the GTV plus a 5 mm margin plus locoregional lymph nodes and neural plexus regions. Planning target volume (PTV) was defined as the CTV with an added margin of at least 5 mm in all directions, modified if OARs were close to the GTV. The gating window was generally defined as a 30% duty cycle around the exhale phase. The mean (\pm standard deviation) GTV displacement at 30% of exhalation for all patients was 2.5 mm (\pm 1.6 mm) in the anterior-posterior direction, 2.1 mm (\pm 1.0 mm) in the lateral direction, and 2.5 mm (\pm 1.6 mm) in the superior-inferior direction. The internal target volume (ITV) was calculated by adding the internal margin derived from 4DCT to the CTV.

Four respiratory-gated treatment plans were generated: a four-field box with passive irradiation (Plan 1) (our present standard technique), four-field scanning irradiation (Plan 2), a three-field (150°, 180°, and 210°) protocol with passive irradiation (Plan 3), and three-field scanning irradiation (Plan 4). The Plan 1 and Plan 2 treatment fraction schemes used three fractions at 0°, two fractions at 90°, four fractions at 180°, and three fractions at 270°. The Plan 3 and Plan 4 scheme used four fractions each at 150°, 180° and 210°. The carbon-ion dose for each plan totaled 55.2 Gy(RBE) in 12 fractions [7]. A patient collimator to reduce blurring of lateral dose distribution was manufactured for each field in passive irradiation, but is not required in scanning irradiation.

Doses were evaluated with regard to dose delivered to 95% of PTV (PTV-D95), dose to the most exposed 2 cc (D2cc) and volume receiving $> n$ Gy(RBE) (V_n Gy(RBE)) of the stomach, duodenum (D1-2: 1st and 2nd portions, D3-4: 3rd and 4th portions) and kidneys, and the maximum dose (Dmax) to the spinal cord. Treatment planning was performed to cover the PTV-D95 with at least 90% of the prescribed dose. The dose

constraints were as follows: 50% of the kidneys' volume should receive < 15 Gy(RBE), a V30 of stomach/D1-2/D3-4 < 5 cc, and a D2cc of the stomach/D1-2/D3-4 < 40 Gy(RBE). The dose to the spinal cord was limited to 30 Gy (RBE). The dose constraints of the OARs were assigned higher priority than target dose coverage. Dose assessment metrics in the respective plans were compared using the Wilcoxon signed-rank test. All p values were two-sided and those < 0.05 were regarded as statistically significant.

RESULTS

A typical dose distribution and DVH for each plan are shown in Figures 1 and 2, respectively. For the four-field box irradiation, Plan 2 increased OAR dose in the range of < 5 Gy(RBE) and decreased dose in the range of ≥ 5 Gy(RBE) in comparison to Plan 1. In Figure 1, cold spots appear in the anterior side of the PTV in Plan 2, because the stomach was cephalad to the PTV; however, it was still at a clinically acceptable level (Plan 1/Plan 2 PTV-D95, 51.6 Gy(RBE)/51.3 Gy(RBE)). For the oblique beam angles, Plan 3 and Plan 4 decreased the dose to the intestinal tract in the range of 10%, but also increased the dose to the spinal cord, kidneys, and vertebral bodies in the range of 10–70%. The dose to the cord exceeded the maximum tolerated dose in Plan 3 (Plan 3/Plan 4 spinal cord Dmax, 51.2 Gy(RBE)/29.7 Gy(RBE); right kidney V10, 113.9 cc/48.1 cc; left kidney V10, 15.1 cc/4.6 cc). The skin dose in Plan 3 was higher than that in Plan 4.

For all the patients, the D95 in all plans was over 90% of the prescribed dose to the PTV (= 49.68 Gy(RBE)) (Table 2). The Plan 3 data were excluded from analysis because all cases in Plan 3 exceeded the maximum allowed dose to the spinal cord. We compared the results for Plans 1, 2, and 4.

Comparing Plan 1 with Plan 2, the PTV coverage remained at a similar level. Plan 2 decreased the V10 of the stomach and duodenum (Plan 1/Plan 2 stomach V10, 88.9 cc/33.9 cc; D1-2 V10, 27.7 cc/12.6 cc; D3-4 V10, 8.1 cc/4.4 cc). Although the V20 of D1-2 was higher in Plan 2, the difference in values was very small and would be clinically insignificant (D1-2 V20, 0.4 cc/0.7 cc). Excepting the D1-2 V20, there was no difference in range of \geq V20 or V30 to the stomach and duodenum. Dmax to the

spinal cord in Plan 2 was lower than that in Plan 1 (Dmax, 18.4 Gy(RBE)/12.3 Gy(RBE)). Plan 2 decreased the dose to both kidneys (right kidney V10, 8.4 cc/0.1 cc; left kidney V10, 25.6 cc/14.2 cc).

As described above, Plan 2 was superior to Plan 1, and Plan 3 resulted in an overdose to the spinal cord. Accordingly, we compared scanning irradiation techniques using Plans 2 and 4. Both plans achieved adequate PTV coverage. Although there were no differences in any range of D3-4 or in the range of \geq V20 of D1-2, Plan 4 decreased D2cc, V20 and V10 to the stomach and V10 to D1-2 (Plan 2/Plan 4 stomach D2cc, 23.1 cc/19.5 cc; V20, 3.1 cc/1.9 cc; V10, 33.9 cc/6.4 cc; D1-2 V10, 12.6 cc/2.2 cc). Dmax to the spinal cord and doses to both kidneys in Plan 4 were higher than those in Plan 2 due to the beam angles, although they remained within an acceptable range.

DISCUSSION

We assessed carbon-ion beam dose planning distributions for pancreatic cancer by comparing passive and scanning irradiation, and four-field box and oblique three-field beam angles. Irrespective of beam angle, scanning irradiation resulted in lower doses to the stomach and duodenum, because scanning irradiation minimizes excessive dose to the normal tissues in front of the target.

The stomach and duodenum received less excessive doses from the passive irradiation in the range of < 5 Gy(RBE) (Figure 2), because the patient collimator used in passive irradiation reduced lateral dose fall-off.

Dose escalation for pancreatic cancer has been studied clinically [8, 9]. The main limiting adverse effect has been upper gastrointestinal toxicity [10]. Tseng et al. assumed that low doses to the stomach were the only significant dosimetric variables correlating with the development of nausea, vomiting, or both. A stomach V10 $\geq 11.5\%$ was the best predictor. In their study, the total proton radiotherapy dose was 25 Gy(RBE) in 5 fractions [11]. Conversely, Nakamura et al. reported that high, rather than low, doses to the stomach caused complications. A V50 ≥ 16 cc and V50 ≥ 33 cc were particularly the best predictors of grade 2 or higher acute gastrointestinal tract and upper gastrointestinal bleeding, respectively. In their study, the total photon radiotherapy dose was 54 Gy in 30 fractions [12]. The dosimetric parameters of

gastrointestinal toxicity are controversial, but the dose to the upper gastrointestinal tract in our present study was below the doses reported in these studies. In our institute, Shinoto et al. reported that when the dose levels of carbon ion radiotherapy were escalated from 43.2 to 55.2 Gy (RBE) in 12 fractions, only 1 of the 72 treated patients experienced a late grade 3 gastric ulcer and bleeding [13].

Gas and peristalsis in the gastrointestinal tract can cause dose distribution variations. Kumagai et al. reported that beam angles in the anterior and left directions could be associated with dose variations due to gas bubble positions, resulting in beam overshoot/undershoot [14]. To solve this problem, it is recommended to irradiate through solid organs, such as the spinal cord and kidneys. Although Plan 3 led to overdose to OARs, Plan 4 met the criteria. Our results indicate that scanning irradiation enables therapy which is less subject to dose irregularities from gas in the digestive tract.

It is reported that intensity-modulated proton therapy (IMPT) has potential advantages in conformity of target coverage and better sparing of normal tissue. Though IMPT may reduce the normal tissue dose and allow further dose escalation compared to IMRT or passive scattering proton therapy [15], additional studies are required because of the risk of multiple inhomogeneous fields due to intra- and inter-fraction motion [16].

Several limitations of our study warrant mention. First, we did not use a field-specific ITV, which considers intrafractional range variations, in this study. This is because most commercial treatment planning systems have not yet implemented the design function of the field-specific ITV. Our pancreatic treatment was applied with respiratory gating to minimize intrafractional motion and 3D treatment planning was not problematic in this study.

Second, we calculated dose distribution using CT images acquired in the supine position only, whereas in practice CT images are acquired in both the supine and prone positions. There is a significant reduction in the movement of the liver and pancreas in the prone position, especially in the superior–inferior direction [17]. The prone position may offer an advantage in radiotherapy in these organs.

Finally, several groups have reported that the interplay effect of residual target motion can still lead to significant underdosing and thus requires further mitigation

techniques such as rescanning, even though gating is applied. Treatment planning would be more realistic when dose distributions are calculated at different respiratory phases with inclusion of the interplay effect (full 4D treatment planning), however, most commercially available treatment planning system cannot do this. Previously, our group reported that four or more phase-controlled rescannings should substantially improve the accuracy of dose conformation [18, 19]. Therefore, we did not consider the interplay effect in this study.

CONCLUSIONS

We found that an oblique three-field scanning irradiation technique was superior to four-field box passive and four-field scanning irradiation. We believe that our results will be helpful for the planning of respiratory-gated scanning irradiation and dose-escalation trials for pancreatic cancer.

REFERENCES

- [1] Siegel R, Ma J, Zou Z, et al. Cancer statistics, 2014. *CA: a cancer journal for clinicians* 2014;64:9-29.
- [2] Bouchard M, Amos RA, Briere TM, et al. Dose escalation with proton or photon radiation treatment for pancreatic cancer. *Radiotherapy and oncology : journal of the European Society for Therapeutic Radiology and Oncology* 2009;92:238-43.
- [3] Nichols RC, Jr., Huh SN, Prado KL, et al. Protons offer reduced normal-tissue exposure for patients receiving postoperative radiotherapy for resected pancreatic head cancer. *International journal of radiation oncology, biology, physics* 2012;83:158-63.
- [4] Suit H, DeLaney T, Goldberg S, et al. Proton vs carbon ion beams in the definitive radiation treatment of cancer patients. *Radiother Oncol* 2010;95:3-22.
- [5] Kamada T. Overview of the Heavy-Ion Medical Accelerator in Chiba (HIMAC) Practices: Tujii H, Kamada T, Shirai T, editors. *Carbon-Ion Radiotherapy* Springer; 2014. p. 17-22.
- [6] Mori S, Shirai T, Takei Y, et al. Patient handling system for carbon ion beam scanning therapy. *J Appl Clin Med Phys* 2012;13:226-40.
- [7] ICRU-72. Prescribing RaRPBTstI, report 78): International Commission on Radiation Units and Measurements. DeLuca P. 2007.
- [8] Komaki R, Wadler S, Peters T, et al. High-dose local irradiation plus prophylactic hepatic irradiation and chemotherapy for inoperable adenocarcinoma of the pancreas. A preliminary report of a multi-institutional trial (Radiation Therapy Oncology Group Protocol 8801). *Cancer* 1992;69:2807-12.
- [9] Ceha HM, van Tienhoven G, Gouma DJ, et al. Feasibility and efficacy of high dose conformal radiotherapy for patients with locally advanced pancreatic carcinoma. *Cancer* 2000;89:2222-9.
- [10] Crane CH, Antolak JA, Rosen II, et al. Phase I study of concomitant gemcitabine and IMRT for patients with unresectable adenocarcinoma of the pancreatic head. *International journal of gastrointestinal cancer* 2001;30:123-32.
- [11] Tseng YD, Wo JY, Ancukiewicz M, et al. Dosimetric predictors of nausea and vomiting: an exploratory analysis of a prospective phase I/II trial with neoadjuvant accelerated short-course radiotherapy and capecitabine for resectable pancreatic cancer. *Journal of Radiation Oncology* 2013;2:427-34.

- [12] Nakamura A, Shibuya K, Matsuo Y, et al. Analysis of dosimetric parameters associated with acute gastrointestinal toxicity and upper gastrointestinal bleeding in locally advanced pancreatic cancer patients treated with gemcitabine-based concurrent chemoradiotherapy. *International journal of radiation oncology, biology, physics* 2012; 84:369-75.
- [13] Shinoto M, Yamada S, Terashima K, et al. Carbon Ion Radiation Therapy With Concurrent Gemcitabine for Patients With Locally Advanced Pancreatic Cancer. *International journal of radiation oncology, biology, physics* 2016; 95:498-504
- [14] Kumagai M, Hara R, Mori S, et al. Impact of intrafractional bowel gas movement on carbon ion beam dose distribution in pancreatic radiotherapy. *International journal of radiation oncology, biology, physics* 2009;73:1276-81.
- [15] Zhang X, Li Y, Pan X, et al. Intensity-modulated proton therapy reduces the dose to normal tissue compared with intensity-modulated radiation therapy or passive scattering proton therapy and enables individualized radical radiotherapy for extensive stage IIIB non-small-cell lung cancer: a virtual clinical study. *International journal of radiation oncology, biology, physics* 2010;77:357-66.
- [16] Lomax AJ. Intensity modulated proton therapy and its sensitivity to treatment uncertainties 2: the potential effects of inter-fraction and inter-field motions. *Physics in medicine and biology* 2008;53:1043-56.
- [17] Kim YS, Park SH, Ahn SD, et al. Differences in abdominal organ movement between supine and prone positions measured using four-dimensional computed tomography. *Radiother Oncol* 2007;85:424-8.
- [18] Mori S, Furukawa T, Inaniwa T, et al. Systematic evaluation of four-dimensional hybrid depth scanning for carbon-ion lung therapy. *Med Phys.*2013;40:031720.
- [19] Mori S, Zenklusen S, Inaniwa T, et al. Conformity and robustness of gated rescanned carbon ion pencil beam scanning of liver tumors at NIRS. *Radiother Oncol* 2014;111:431-6.

Table 1

Patient characteristics.

UICC Stage grouping: Stage IIA: T3, N0, M0; Stage III: T4, Any N, M0; Stage IV: Any T, Any N, M1

Characteristics		
Number of patients		13
Age, years		
	Median (range)	63 (35 - 80)
Gender		
	Male	8
	Female	5
PS		
	0	12
	1	1
Stage (UICC 7th)		
	II A	2
	III	8
	IV	3
Tumor location		
	Head	6
	Body/tail	7
GTV size, cc		
	Median (range)	13.9 (1.7 -47.4)
CA19-9, U/ml		
	Median (range)	684.5 (0.1 - 6560)

Table 2

Dose assessment for all patients.

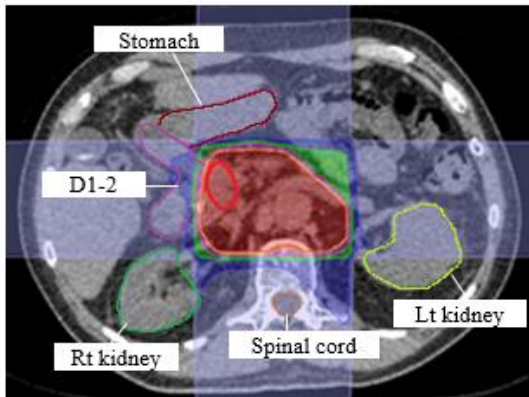
Abbreviations: PTV, planning target volume; D95, dose delivered to 95% of the irradiated volume; Dmax, maximum dose; V_n, volume receiving > n Gy(RBE); D1-2, 1st and 2nd portions of duodenum; D3-4, 3rd and 4th portions of duodenum; P 1, Plan 1; P 2, Plan 2; P 4, Plan 4; range*, interquartile range.

	Plan 1	Plan 2	Plan 3	Plan 4	P 1 vs P 2	P 2 vs P 4
	passive	scanning	passive	scanning	p values	p values
	median (range*)	median (range*)	median (range*)	median (range*)		
PTV						
D95, Gy (RBE)	51.8 (51.6-52.2)	51.3 (51.3-51.5)	51.8 (51.2-51.9)	51.4 (51.2-52.0)	0.16	0.95
Stomach						
D2cc, Gy (RBE)	25.2 (19.9-28.8)	23.1 (21.0-27.5)	8.9 (8.2-16.9)	19.5 (18.1-24.7)	0.67	<0.01
V30, cc	0.3 (0.2-1.6)	0.6 (0.5-1.4)	0.0 (0.0-0.2)	0.7 (0.4-1.2)	0.20	0.75
V20, cc	4.8 (2.0-14.9)	3.1 (2.4-5.5)	0.2 (0.1-1.3)	1.9 (1.7-3.2)	0.07	<0.01
V10, cc	88.9 (71.6-112.0)	33.9 (20.7-38.0)	3.2 (0.8-3.8)	6.4 (4.8-8.3)	<0.01	<0.01
D1-2						
D2cc, Gy (RBE)	15.9 (15.4-19.3)	12.2 (10.9-15.9)	19.0 (2.6-19.5)	15.6 (8.3-19.4)	0.05	0.46
V30, cc	0.1 (0.0-0.5)	0.2 (0.0-0.7)	0.0 (0.0-0.3)	0.1 (0.1-0.7)	0.07	0.81
V20, cc	0.4 (0.1-1.8)	0.7 (0.3-2.1)	1.1 (0.3-2.5)	0.9 (0.4-1.9)	<0.01	0.38
V10, cc	27.7 (22.8-31.0)	12.6 (9.5-15.8)	6.0 (0.9-9.5)	2.2 (1.3-7.2)	<0.01	<0.01
D3-4						
D2cc, Gy (RBE)	13.3 (9.8-23.6)	17.2 (11.7-20.9)	9.0 (2.1-21.6)	13.2 (11.4-20.3)	0.72	0.14
V30, cc	0.2 (0.1-0.7)	0.6 (0.3-0.8)	0.2 (0.0-0.9)	0.6 (0.1-1.0)	0.05	0.73
V20, cc	1.4 (0.4-2.7)	1.5 (0.9-2.2)	0.6 (0.3-2.3)	1.3 (0.7-2.0)	0.75	0.36
V10, cc	8.1 (1.9-14.0)	4.4 (2.3-6.1)	2.1 (0.8-4.5)	3.1 (2.3-8.4)	<0.05	0.29
Spinal cord						
Dmax, Gy (RBE)	18.4 (16.7-19.8)	12.3 (11.7-13.0)	51.2 (47.3-52.6)	27.9 (26.9-28.7)	<0.01	<0.01
Rt kidney						
D2cc, Gy (RBE)	14.6 (8.0-20.0)	8.7 (4.3-15.5)	17.2 (13.3-27.2)	11.0 (9.5-28.2)	<0.01	<0.01
V30, cc	0.0 (0.0-0.2)	0.0 (0.0-0.4)	0.0 (0.0-0.2)	0.0 (0.0-1.4)	0.31	0.05
V20, cc	0.0 (0.0-2.0)	0.0 (0.0-1.2)	0.0 (0.0-4.6)	0.0 (0.0-10.5)	0.22	0.05
V10, cc	8.4 (1.6-17.6)	0.1 (0.0-4.8)	36.7 (21.4-94.7)	4.0 (1.1-43.1)	<0.01	<0.01
Lt kidney						
D2cc, Gy (RBE)	22.4 (13.6-27.0)	23.4 (11.4-25.6)	46.4 (27.4-53.3)	33.5 (21.6-38.0)	0.16	<0.01
V30, cc	0.8 (0.1-1.5)	1.0 (0.3-1.2)	12.7 (1.4-14.5)	3.2 (0.7-5.8)	0.65	<0.01
V20, cc	3.9 (0.6-11.9)	2.3 (0.8-2.6)	19.6 (4.6-25.7)	9.9 (2.7-14.8)	<0.05	<0.01
V10, cc	25.6 (12.6-32.3)	14.2 (2.6-16.9)	69.9 (60.1-95.3)	37.0 (20.5-57.3)	<0.01	<0.01

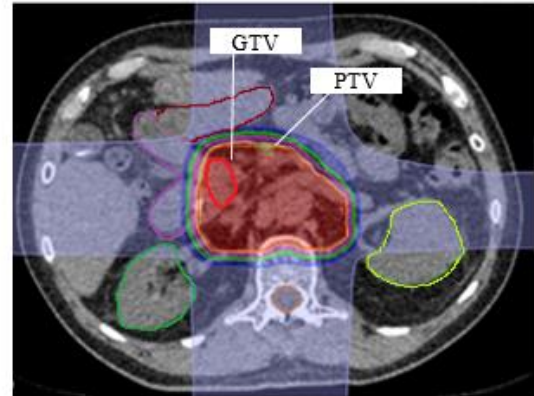
Figure 1

Carbon-ion dose distributions in axial (patient no. 10) for (a) Plan 1, (b) Plan 2, (c) Plan 3 and (d) Plan 4.

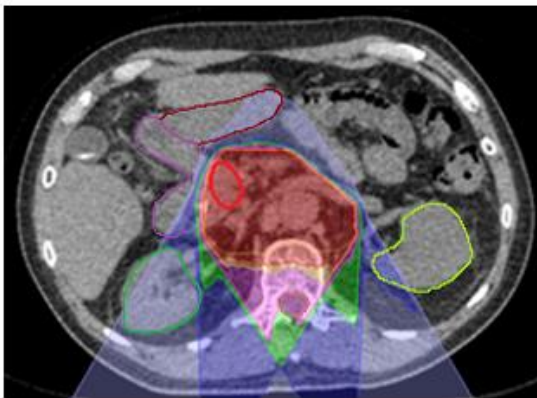
Red and yellow lines show gross tumor volume (GTV) and planning target volume (PTV), respectively. Red, yellow, pink, green, dark blue, and light blue isodose lines show 95%, 90%, 70%, 50%, 30%, and 10% of the prescribed dose, respectively.



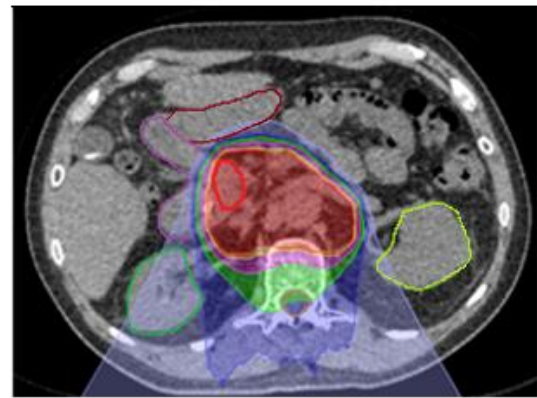
(a) Plan 1



(b) Plan 2



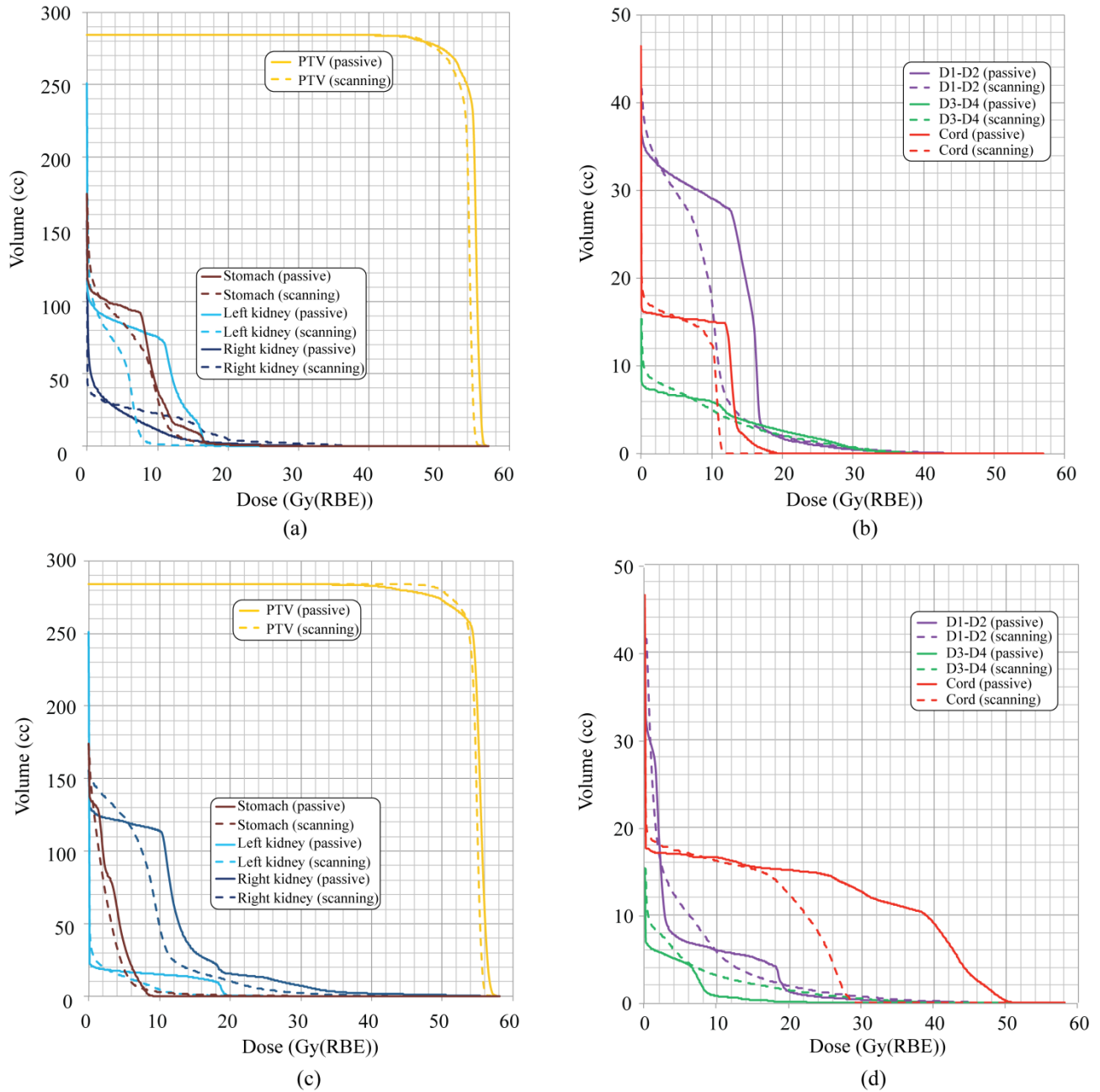
(c) Plan 3



(d) Plan 4

Figure 2

Dose-volume histograms for (a)–(b): four-field box irradiation and (c)–(d): oblique beam irradiation (patient no. 10).



Radiotherapy and Oncology Vol.119 No.2

平成 28 年 6 月 1 日 公表済